

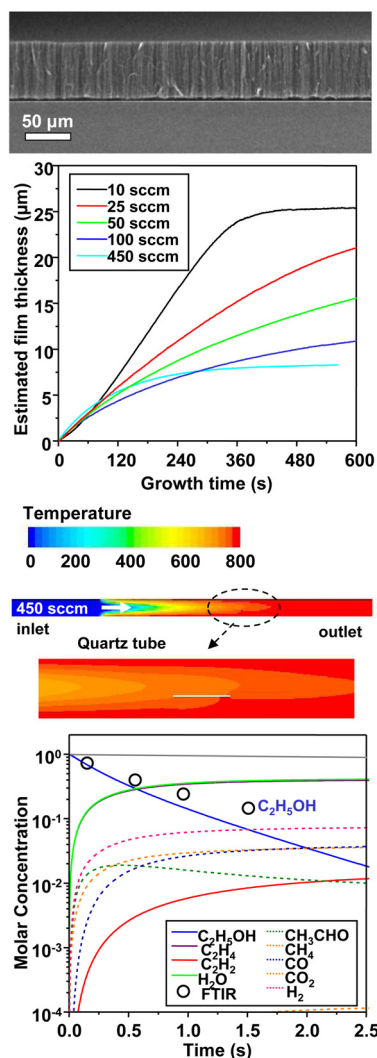
# Parametric study of ACCVD for controlled synthesis of vertically aligned single-walled carbon nanotubes

Rong Xiang<sup>1</sup>, Erik Einarsson<sup>1</sup>, Jun Okawa<sup>1</sup>, Theerapol Thurakitserree<sup>1</sup>, Yoichi Murakami<sup>2</sup>, Junichiro Shiomi<sup>1</sup>, Yutaka Ohno<sup>3</sup>, Shigeo Maruyama<sup>1\*</sup>

<sup>1</sup>Department of Mechanical Engineering, The University of Tokyo, Tokyo 113-8656, Japan

<sup>2</sup>Department of Chemical System Engineering, The University of Tokyo, Tokyo 113-8656, Japan

<sup>3</sup>Department of Quantum Engineering, Nagoya University, Nagoya 464-8603, Japan



# Parametric study of ACCVD for controlled synthesis of vertically aligned single-walled carbon nanotubes

Rong Xiang<sup>1</sup>, Erik Einarsson<sup>1</sup>, Jun Okawa<sup>1</sup>, Theerapol Thurakitseree<sup>1</sup>, Yoichi Murakami<sup>2</sup>,  
Junichiro Shiomi<sup>1</sup>, Yutaka Ohno<sup>3</sup>, Shigeo Maruyama<sup>1\*</sup>

<sup>1</sup>Department of Mechanical Engineering, The University of Tokyo, Tokyo 113-8656, Japan

<sup>2</sup>Department of Chemical System Engineering, The University of Tokyo, Tokyo 113-8656, Japan

<sup>3</sup>Department of Quantum Engineering, Nagoya University, Nagoya 464-8603, Japan

In this study we examine catalyst preparation and chemical vapor deposition parameters related to synthesis of single-walled carbon nanotubes (SWNTs) by alcohol catalytic CVD. We show that modifying the catalyst recipe considerably changes the average SWNT diameter, and vertically aligned arrays with an average diameter of 1.5 nm were obtained. The height of vertically aligned SWNT arrays can be significantly enhanced by surface modification of the substrate prior to dip-coating, although this produces SWNTs with larger diameters at the root of the array. We demonstrate patterned growth by combining this method with suppression of SWNT synthesis by formation of a hydrophobic surface. We also consider the effects of ethanol flow rate and thermal decomposition on the chemical environment at the substrate. The growth process is considerably altered by the extent of ethanol decomposition, with sudden termination of the growth occurring in the extreme low-flow (complete decomposition) case.

**Keywords:** Nanotube, SWNT, Alcohol CVD, Synthesis.

\*Corresponding Author: maruyama@photon.t.u-tokyo.ac.jp, Tel/Fax: +81-3-5800-6983

## Introduction

Synthesis of vertically aligned single-walled carbon nanotubes (VA-SWNTs) was first reported<sup>1</sup> in early 2004 using a technique based on alcohol catalytic chemical vapor deposition (ACCVD).<sup>2</sup> Many other methods were developed soon after, such as water-assisted,<sup>3</sup> oxygen-assisted,<sup>4</sup> microwave plasma,<sup>5</sup> and molecular beam<sup>6</sup> synthesis. Among these methods, the ACCVD method is arguably the simplest, and unique in that the catalyst can be applied by various methods such as the original dip-coating method<sup>7</sup> and combinatorial sputtering deposition.<sup>8</sup> In this paper, we use a solution-based dip-coating method<sup>7</sup> that has been shown to produce monodisperse nanoparticles<sup>10</sup> with diameters of approximately 2 nm. Some advantages of this wet approach include deposition of a very small amount of metal catalyst, as well as excellent potential for low-cost scalability. However, this method has thus far failed to provide full control over the morphology of the produced SWNTs due to insufficient understanding of the process. In this report we extend this wet process to tailor the key structural parameters of the SWNTs array, including diameter, length, and growth location of the SWNTs. Specifically, our liquid based catalyst preparation is also found to be powerful in tailoring the diameter of the grown SWNTs, producing the narrowest-diameter VA-SWNTs yet reported. The substrate wettability is found to be critical for the yield of SWNTs. On an OH-terminated hydrophilic Si/SiO<sub>2</sub> surface, the growth can be promoted by 10 times, but can be completely suppressed on a CH<sub>3</sub>-terminated hydrophobic surface. Selective surface modification is also utilized to localize the growth of SWNTs. The proposed technique has advantages in improved simplicity and potentially better resolution compared to conventional lithography. Related to our previous finding that no-flow ACCVD is suited for growth of longer VA-SWNTs,<sup>11</sup> some updated understanding of the decomposition of ethanol in ACCVD is also presented.

## Experimental procedures

The SWNT arrays used in this study were synthesized by the ACCVD method,<sup>2</sup> where cobalt and molybdenum nanoparticles were loaded onto a silicon or quartz substrate by a liquid-based dip-coat method.<sup>7</sup> The details and procedures have been described in previous reports,<sup>1, 12, 13</sup> but essentially involve two dip-coating steps—once in a Mo solution, and once in a Co solution— followed by low-pressure alcohol CVD at 700-800 °C. Each dip-coat step is followed by calcinations in air for 5 min at 500 °C. Synthesis by this method has been shown to be a root-growth process,<sup>14</sup> with catalyst nanoparticles remaining on the substrate surface and SWNTs growing perpendicular to the substrate. The growth process has been investigated using an *in situ* optical absorbance measurement,<sup>12</sup> which shows the growth rate decays exponentially from an initial maximum.<sup>15</sup> The resulting VA-SWNT arrays typically have a thickness of 10-30 μm, and consist of small bundles of ten or fewer SWNTs.<sup>16</sup> The diameters range from 0.8 to 3.0 nm, with an average diameter of 2.0 nm.<sup>17</sup> Carbon may be better]Our standard synthesis conditions are 800 °C and 1.4 kPa (10 Torr) of ethanol at a flow rate of 450 sccm. Standard catalyst concentrations are 0.01 wt% of both Mo and Co. The catalyst nanoparticles are reduced under 40 kPa (300 Torr) of 3% H<sub>2</sub> (Ar balance) during heating of the CVD chamber, but the Ar/H<sub>2</sub> flow is stopped prior to the introduction of ethanol.

## Controlling average diameter

It is highly desirable to have control over the diameter of a synthesized SWNT because its diameter determines its electrical and optical band gap and affects many other properties. In some applications, particularly those utilizing optical properties of SWNTs such as a mode-locked fiber laser,<sup>18, 19</sup> the average diameter of the SWNTs may need to be tuned to optimize performance. In this work we investigate the effect in catalyst preparation methods on the average nanotube diameter, and compare with the influence of CVD parameters such as temperature and pressure. Figure 1(a) shows absorbance spectra for identically prepared substrates that were grown at different temperatures and ethanol pressures. Here we use optical absorption because it provides information on the entire ensemble without being selective like photoluminescence and Raman spectroscopy. For

samples synthesized at 800 °C and different ethanol pressures, the positions of the  $E_{11}$  and  $E_{22}$  peaks shift very slightly, showing a weak dependence of diameter on the ethanol pressure. The average diameter can be reduced slightly by decreasing the synthesis temperature<sup>20</sup> (topmost blue curve), but overall the average diameter is weakly dependent on the synthesis temperature and is almost completely independent of ethanol pressure. Based on these results, very little control over the diameter is possible by changing CVD parameters. The SWNT diameter was found to be much more sensitive to catalyst preparation methods, as shown in Fig. 1(b). The middle (green) spectrum corresponds to our standard procedure, as described above. Decreasing the catalyst concentration to 1% of the standard case (lower violet curve) produced SWNTs with an average diameter of 1.5 nm, 25% smaller than in the standard case. On the other hand, increasing the calcination time after dip-coating (upper pink curve) considerably increased the average SWNT diameter, showing that the diameter may be adjusted over a wide range by changing the catalyst recipe. This trend is similar to that found in a previous comprehensive work on diameter control.<sup>21</sup> However, the current catalyst preparation method is less complicated and, more importantly, resulted in smaller-diameter SWNTs (1.5 nm). A TEM micrograph of these SWNTs is shown in Fig. 1(c). Such small-diameter VA-SWNTs would be more useful in optical devices.

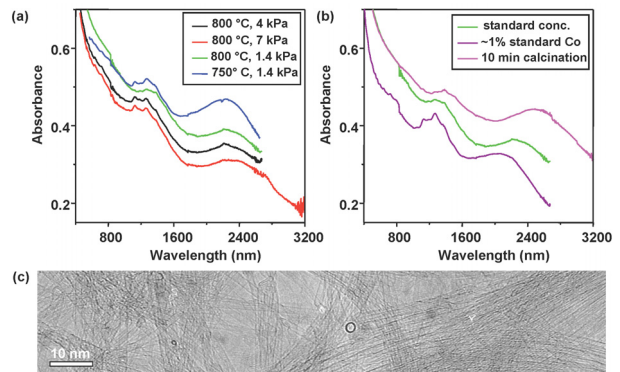


Fig. 1 (a) UV-Vis-NIR absorption spectra of SWNT arrays grown at different pressures and temperatures. Substrate was tilted by 30 deg. (b) Effect of catalyst condition on optical absorption. (c) A typical TEM image of SWNTs with an average diameter of 1.5 nm, obtained by controlling the concentration of the catalyst precursor in the dip-coating solution.

### Increasing SWNT length

Although the typical height of our VA-SWNT arrays is approximately 10  $\mu\text{m}$ , much taller arrays can be obtained by several approaches. We found that the decomposition of ethanol<sup>9</sup> is critically important for this growth process. The detailed and practical analysis of the decomposition of ethanol is discussed in the last section of this paper.

An alternative method is the modification of the substrate surface chemistry. Figure 2(a) shows a 150  $\mu\text{m}$  VA-SWNT array synthesized under the aforementioned standard CVD conditions. This was achieved by exposing the substrate to  $\text{O}_2$  plasma prior to dip-coating, which resulted in the surface of Si/SiO<sub>2</sub> substrate being terminated by a carboxyl group. Since the OH-terminated surface is more hydrophilic than an as-delivered, clean, untreated surface, our first speculation was that perhaps more catalyst was loaded onto the surface due to the increased hydrophilicity. However, simply increasing the concentration of the catalyst in the dip-coating solutions and using an un-

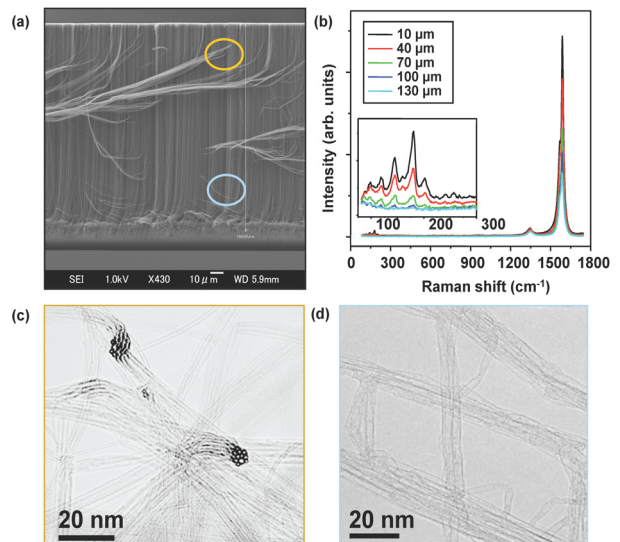


Fig. 2 (a) SEM image of a VA-SWNT array with thickness of 150  $\mu\text{m}$  obtained by pre-treating the SiO<sub>2</sub> substrate with oxygen plasma prior to dip-coating; (b) resonance Raman spectra (488 nm excitation) from different positions along the array, showing a intensity decrease in G-band and RBM peaks; typical

treated surface resulted in no significant growth promotion. We believe this is because of the chemisorbed state of our metal acetate molecules onto specific surface sites.<sup>10</sup> The surface concentration of metal atoms is very weakly dependent on the concentration of the solution, as seen in Fig. 1(b) where the concentration was changed by two orders of magnitude.

Although more investigation is needed to clarify the mechanism, we hypothesize that particles loaded onto the OH-terminated surface are more likely to migrate and agglomerate into larger particles (perhaps due to a higher catalyst density). This is evidenced by further characterization of the detailed structure of these tall arrays. Figure 2 (b) shows resonance Raman spectra obtained from different positions along the height of the array. The intensity of the G-band and RBM peaks get considerably weaker toward the bottom of the array, while the intensity of the D-band is essentially unchanged. TEM observations show the SWNTs at the top of the array (Fig. 2(c)) are considerably smaller than near the bottom (Fig. 2(d)), suggesting significant catalyst aggregation or ripening during growth. Although at this stage there is no direct evidence confirming the relationship between catalyst diameter and catalyst lifetime, empirically all reported ultra-long SWNTs seem to have large (e.g. ~4nm) average diameters. The ability to form very tall SWNT arrays may be dependent on sufficiently large catalyst particles. Since tall, larger diameter SWNT arrays have many potential applications where large quantity or easy manipulation is required,<sup>22</sup> clarifying the catalytic conditions necessary for such growth is important to tailor VA-SWNT arrays to match a target application.

### Localization of SWNT growth

The effects of surface chemistry on the yield of SWNTs suggest the ability to control the growth position, which is critical to constructing 3-D vertically aligned SWNT structures or 2D SWNT patterns on a substrate. To selectively suppress growth we created the opposite effect of plasma treatment, i.e. increased the hydrophobicity of the surface, by forming a self-assembled monolayer (SAM) of octadecyltrichlorosilane (OTS) on the substrate surface.<sup>23</sup> The terminating  $\text{CH}_3$  group makes the surface superhydrophobic, increasing the contact angle of water from nearly 0 (for OH-terminated) to approximately  $110^\circ$  (not shown). After dip-coating and CVD, almost no carbon structures were found on the substrate. The effects of these surface treatments are compared in Fig. 3(a), which shows that an OH-terminated surface significantly boosted the array height, while a  $\text{CH}_3$ -terminated surface effectively prevented SWNT synthesis.

Patterned growth can be realized by selectively removing the SAM prior to dip-coating, thus depositing catalyst in specified locations. Figure 3(b) shows a scanning electron microscope (SEM) image of such patterned growth. This was achieved by selectively removing the SAM by exposure to UV irradiation through a photomask prior to dip-coating and CVD.<sup>24</sup> SWNTs were only obtained in the regions where the SAM had been removed, i.e. the hydrophilic regions. This shows the potential to predetermine the SWNT growth location using wet chemical methods rather than more complicated conventional lithographic methods. The primary advantage of this surface modification technique is that a wet chemistry approach is a simpler and less expensive fabrication method. Furthermore, selective removal of the SAM has the potential for high-resolution patterning. This is because developing and removal of the photoresist is essentially what limits the resolution of conventional lithography, but both of these steps are bypassed in the current technique. Using the SAM method the resolution limit is

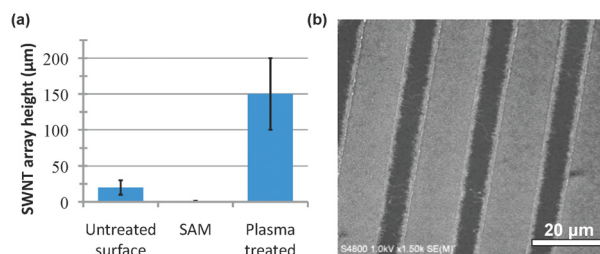


Fig. 3 (a) Surface dependence of VA-SWNT array height. Typical range shown by error bars. (b) SEM image of patterned SWNT growth using selective surface treatment.

determined by how precisely the SAM can be removed, making this a very promising method for obtaining pattern resolution better than 100 nm.

### Thermal decomposition of ethanol

We have previously investigated the influence of CVD temperature and pressure on the synthesis of VA-SWNTs by ACCVD.<sup>15</sup> However, since ethanol thermally decomposes at typical growth temperatures,<sup>25</sup> the actual catalyst environment can be significantly affected by the gas flow rate, even when the furnace temperature is unchanged. Figure 4(a) shows the temperature profile based on a numerical calculation using the FLUENT software package for an ethanol flow rate of 450 sccm through a 60 cm furnace maintained at a temperature of 800 °C. The dashed oval indicates the position of the substrate, and is found to be approximately 20 °C cooler than the furnace temperature. Thermal decomposition of ethanol under these conditions was also calculated, and the concentrations of ethanol and various chemical species produced by its thermal decomposition are shown in Fig. 4(c). Under these conditions, ethanol almost completely decomposes in 2.5 seconds. The residence time in the chamber, however, is only 0.1 s, thus the ethanol concentration near the catalyst should be more than 90%. In the case of a slower flow rate the gas would be heated to the furnace temperature by the time it arrives at the substrate (due to the shorter entrance length), thus slightly increasing the local temperature at the catalyst. Much more importantly, a slower flow would increase the residence time of ethanol in the heated region. As a result, a more significant portion of the ethanol would have thermally decomposed before reaching the catalyst. This is evidenced experimentally by the growth curves presented in Fig. 4(b), which correspond to different ethanol flow rates under otherwise identical conditions. As the flow rate decreases the catalyst lifetime increases significantly, enhancing SWNT growth. This is likely due to an increase in the production of C<sub>2</sub>H<sub>4</sub> and H<sub>2</sub>O. In most cases the general growth behavior is typical exponential decay,<sup>15</sup> but when the flow rate is very slow (i.e., <25 sccm) the growth process changes significantly, as shown by the topmost black curve in Fig. 4(b). In this case the growth rate is nearly constant for approximately three minutes and then suddenly stops. This catalytic sudden-death has been reported elsewhere,<sup>26-28</sup> but the mechanism still remains as an open question in this field.

### Conclusion

In conclusion, we address several issues regarding understanding and controlling the growth of vertically aligned SWNTs synthesized from ethanol. We show it is possible via surface treatment of the substrate to significantly enhance or suppress SWNT growth. Combining these surface treatment methods, area-selective surface treatment was found to be a simple, scalable way to pattern VA-SWNT growth when loading catalyst by a wet dip-coating technique. Characterization indicates that tall (>100 μm) arrays resulting from dip-coating onto OH-terminated surfaces have quite large diameters at the root compared to the top, which indicates significant catalyst aggregation or ripening is occurring during growth. The average diameter of the SWNTs was also found to be dependent on the catalyst concentration, illustrating the flexibility of our method to synthesize SWNTs with various diameters and lengths in a controllable fashion. However, due to the thermal decomposition of ethanol at

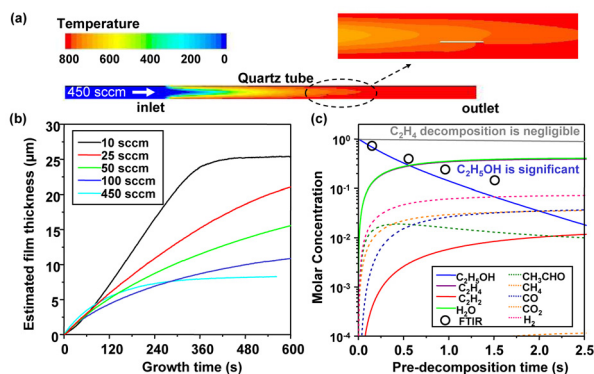


Fig. 4 (a) Temperature distribution inside the quartz tube during CVD. (b) Growth curves at 800 °C for different ethanol flow rates show a change for slow flow rates. (c) Ethanol decomposition curves calculated by CHEMKIN, and experimentally measured ethanol concentrations (circles) by FTIR spectroscopy.

CVD synthesis temperatures, one must also take into account the ethanol flow rate, which determines the chemical environment at the catalyst.

## Acknowledgements

Part of this work was financially supported by Grant-in-Aid for Scientific Research (19206024 and 19054003) from the Japan Society for the Promotion of Science, SCOPE (051403009) from the Ministry of Internal Affairs and Communications, NEDO (Japan), and MITI's Innovation Research Project on Nanoelectronics Materials and Structures, and by Global COE Program 'Global Center for Excellence for Mechanical Systems Innovation', MEXT, Japan.

## References

1. Y. Murakami, S. Chiashi, Y. Miyauchi, M. H. Hu, M. Ogura, T. Okubo, S. Maruyama, *Chem. Phys. Lett.* 385, 298 (2004).
2. S. Maruyama, R. Kojima, Y. Miyauchi, S. Chiashi, M. Kohno, *Chem. Phys. Lett.* 360, 229 (2002).
3. K. Hata, D. N. Futaba, K. Mizuno, T. Namai, M. Yumura, S. Iijima, *Science* 306, 1362 (2004).
4. G. Y. Zhang, D. Mann, L. Zhang, A. Javey, Y. M. Li, E. Yenilmez, Q. Wang, J. P. McVittie, Y. Nishi, J. Gibbons, H. J. Dai, *Proc. Natl. Acad. Sci. U.S.A.* 102, 16141 (2005).
5. G. F. Zhong, T. Iwasaki, K. Honda, Y. Furukawa, I. Ohdomari, H. Kawarada, *Jpn. J. Appl. Phys.* 44, 1558 (2005).
6. G. Eres, A. A. Kinkhabwala, H. Cui, D. B. Geohegan, A. A. Puretzky, D. H. Lowndes, *J. Phys. Chem. B* 109, 16684 (2005).
7. Y. Murakami, Y. Miyauchi, S. Chiashi, S. Maruyama, *Chem. Phys. Lett.* 377, 49 (2003).
8. S. Noda, H. Sugime, T. Osawa, Y. Tsuji, S. Chiashi, Y. Murakami, S. Maruyama, *Carbon* 44, 1414 (2006).
9. H. Sugime, S. Noda, S. Maruyama, Y. Yamaguchi, *Carbon* 47, 234 (2009).
10. M. H. Hu, Y. Murakami, M. Ogura, S. Maruyama, T. Okubo, *J. Catal.* 225, 230 (2004).
11. H. Oshima, Y. Suzuki, T. Shimazu, S. Maruyama, *Jpn. J. Appl. Phys.* 47, 1982 (2007).
12. S. Maruyama, E. Einarsson, Y. Murakami, T. Edamura, *Chem. Phys. Lett.* 403, 320 (2005).
13. E. Einarsson, M. Kadowaki, K. Ogura, J. Okawa, R. Xiang, Z. Zhang, Y. Yamamoto, Y. Ikuhara, S. Maruyama, *J. Nanosci. Nanotechnol.* 8, 6093 (2008).
14. R. Xiang, Z. Zhang, K. Ogura, J. Okawa, E. Einarsson, Y. Miyauchi, J. Shiomi, S. Maruyama, *Jpn. J. Appl. Phys.* 47, 1971 (2008).
15. E. Einarsson, Y. Murakami, M. Kadowaki, S. Maruyama, *Carbon* 46, 923 (2008).
16. E. Einarsson, H. Shiozawa, C. Kramberger, M. H. Rummeli, A. Grüneis, T. Pichler, S. Maruyama, *J. Phys. Chem. C* 111, 17861 (2007).
17. R. Xiang, Z. Yang, Q. Zhang, G. H. Luo, W. Z. Qian, F. Wei, M. Kadowaki, E. Einarsson, S. Maruyama, *J. Phys. Chem. C* 112, 4892 (2008).
18. Y.-W. Song, E. Einarsson, S. Yamashita, S. Maruyama, *Opt. Lett.* 32, 1399 (2007).
19. Y.-W. Song, S. Yamashita, S. Maruyama, *Appl. Phys. Lett.* 92, 021115 (2008).
20. Y. H. Miyauchi, S. H. Chiashi, Y. Murakami, Y. Hayashida, S. Maruyama, *Chem. Phys. Lett.* 387, 198 (2004).
21. T. Yamada, T. Namai, K. Hata, D. N. Futaba, K. Mizuno, J. Fan, M. Yudasaka, M. Yumura, S. Iijima, *Nature Nanotechnol.* 1, 131 (2006).
22. B. Zhao, D. N. Futaba, S. Yasuda, M. Akoshima, T. Yamada, K. Hata, *ACS Nano* 3, 108 (2009).
23. A. Ulman, *Chemical Reviews* 96, 1533 (1996).
24. S. Onclin, B. J. Ravoo, D. N. Reinhoudt, *Angew. Chem.* 44, 6282 (2005).

25. R. Xiang, E. Einarsson, J. Okawa, Y. Miyauchi, S. Maruyama, *J. Phys. Chem. C*, in press.
26. R. Andrews, D. Jacques, D. Qian, T. Rantell, *Acc. Chem. Res.* 35, 1008 (2002).
27. E. R. Meshot, A. J. Hart, *Appl. Phys. Lett.* 92, 113107 (2008).
28. D. B. Geohegan, A. A. Puretzky, I. N. Ivanov, S. Jesse, G. Eres, J. Y. Howe, *Appl. Phys. Lett.* 83, 1851 (2003).